



Transcriptomic and proteomic feature of salt stress-regulated network in Jerusalem artichoke (*Helianthus tuberosus* L.) root based on de novo assembly sequencing analysis

Aiqin Zhang¹ · Dongming Han¹ · Yu Wang² · Huifang Mu¹ · Tong Zhang³ · Xiufeng Yan¹ · Qiuying Pang¹

Received: 21 September 2017 / Accepted: 18 November 2017 / Published online: 28 November 2017
© Springer-Verlag GmbH Germany, part of Springer Nature 2017

Abstract

Main Conclusion Ribosome activation and sugar metabolic process mainly act on the regulation of salt tolerance in the bioenergy crop *Helianthus tuberosus* L. as dissected by integrated transcriptomic and proteomic analyses.

Helianthus tuberosus L. is an important halophyte plant that can survive in saline–alkali soil. It is vitally necessary to build an available genomic resource to investigate the molecular mechanisms underlying salt tolerance in *H. tuberosus*. De novo assembly and annotation of transcriptomes were built for *H. tuberosus* using a HiSeq 4000 platform. 293,823 transcripts were identified and annotated into 190,567 unigenes. In addition, iTRAQ-labeled quantitative proteomics was carried out to detect global protein profiling as a response to salt stress. Comparative omics analysis showed that 5432 genes and 43 proteins were differentially expressed in *H. tuberosus* under salt stress, which were enriched in the following processes: carbohydrate metabolism, ribosome activation and translation, oxidation–reduction and ion binding. The reprogramming of transcript and protein works suggested that the induced activity of ribosome and sugar signaling may endue *H. tuberosus* with salt tolerance. With high-quality sequencing and annotation, the obtained transcriptomics and proteomics provide a robust genomic resource for dissecting the regulatory molecular mechanism of *H. tuberosus* in response to salt stress.

Keywords Energy crop · iTRAQ labeling · RNA-Seq transcriptome · Salt tolerance

Abbreviations

DEPC	Diethyl pyrocarbonate
DEGs	Differentially expressed genes
FPKM	Fragments per kilobase per transcript per million mapped reads
MDHAR	Monodehydroascorbate reductase

LEA	Late embryogenesis abundant
RSEM	RNA-seq by expectation maximization

Introduction

Soil salinization is one of the major abiotic stresses affecting plant growth and menacing agricultural productivity, which has spread continuously in most areas of the world (Zhu 2001; Yamaguchi and Blumwald 2005). *Helianthus tuberosus* L., an important sunflower plant that can survive in saline–alkali soil and semiarid climate, has also been cultivated as a vegetable, fodder crop and a source for bioenergy production in many countries owing to its enrichment in polysaccharides, especially inulin (Wright et al. 1977; Zhao et al. 2006; Barta and Pátkai 2007; Long et al. 2010a, b). Previous studies have demonstrated that various storage carbohydrates in the tubers offer *H. tuberosus* seedlings the capacity to thrive under environmental stresses, such as drought and salt (Saengthongpinit and Sajjaanantakul 2005; Valluru and Van Den Ende 2008).

Electronic supplementary material The online version of this article (<https://doi.org/10.1007/s00425-017-2818-1>) contains supplementary material, which is available to authorized users.

✉ Qiuying Pang
qiuying@nefu.edu.cn

¹ Alkali Soil Natural Environmental Science Center, Northeast Forestry University/Key Laboratory of Saline-alkali Vegetation Ecology Restoration, Ministry of Education, Harbin 150040, China

² School of Life Science and Technology, Harbin Institute of Technology, Harbin 150080, China

³ Department of Biology, University of Florida, Gainesville, FL 32610, USA

Originated in central-eastern North America where the wild populations abound, *H. tuberosus* is a hexaploid plant with 102 chromosomes ($2n = 66^* = 102$) (Rogers et al. 1982; Kays and Nottingham 2008). Genome skimming provided genetic evidence that *H. tuberosus* originated recursively from perennial sunflowers via hybridization between tetraploid hairy sunflower and diploid sawtooth sunflower (Bock et al. 2014). The largest genome size of *Helianthus* plants can reach up to 3600 Mb, and newly formed plant polyploids may undergo extensive genomic changes; therefore the size of *H. tuberosus* genome is still unpredictable (Baack et al. 2005). Until now, limited genomic resources are available for *H. tuberosus*. There are only 40,362 ESTs, 1281 protein sequences deposited in the NCBI genebank and one de novo transcriptome sequencing work on *H. tuberosus*. However, only 272,548 transcripts were assembled due to low read length and the inherent limitations of the sequencing platform used (Jung et al. 2014). It is clearly insufficient to establish the genetic and molecular knowledge of *H. tuberosus* based on the formidable genome, especially the molecular mechanism of its high adversity resistance.

Several investigations have been conducted to characterize the physiological responses of *H. tuberosus* to salt stress. It has been shown that resistance to salt stress in *H. tuberosus* can be achieved by osmotic adjustment, selective ion absorption and activation of the antioxidant system (Chen et al. 2011; Huang et al. 2012, 2013). However, a mechanistic understanding of the molecular regulation networks to salt stress is still lacking, given the scarce availability of genetic information of *H. tuberosus*. In addition, all previous studies have focused on the analysis of leaves in salt tolerance of *H. tuberosus* and the contribution of roots has been largely ignored (Long et al. 2010a, b; Huang et al. 2013). The ability of the underground system of *H. tuberosus* to withstand a high level of salt and to support plant growth is mostly due to the characteristic fibrous thin cord-like rhizomes, which acquire plenty of storage energy from tubers (Ma et al. 2011).

To shed light on the molecular mechanisms underlying salt tolerance in *H. tuberosus*, we used root tissues to assemble and annotate a reference transcriptome with a high-performance HiSeq 4000 platform to identify the global gene expression changes. Further investigation was carried out by iTRAQ-labeled proteome to detect differentially expressed proteins under salt stress. This study would provide rich information to explore the molecular toolbox and define the primary regulatory mechanisms of *H. tuberosus* in response to salt stress.

Materials and methods

Plant growth, salt treatment and tissue collection

Tubers of *H. tuberosus* were collected from a saline–alkali soil area located in Zhaodong, Heilongjiang Province,

China. After washing with distilled water, the tubers were planted in plastic pots filled with aseptic vermiculite and fertile black soil (2:1, v/v). Plants were grown in a greenhouse at 25/20 °C (day/night) with a 8 h light/16 h dark photoperiod, photosynthetically active radiation $150 \text{ mol m}^{-2} \text{ s}^{-1}$ and 50–70% relative humidity and were irrigated daily by half-strength Hoagland's solution (pH 6.21 ± 0.10) with or without 50, 150 or 250 mM NaCl. Root tissues from the control and salt-treated samples were collected at 15 days after sowing when the seedling reached approximately 10 cm height. The root tissues were washed with distilled water, followed by surface drying with filter paper. Harvested tissues were either frozen in liquid nitrogen and stored at $-80 \text{ }^\circ\text{C}$ until further analysis or used immediately.

Na⁺ and K⁺ content analysis

The collected samples were oven dried at 80 °C to a constant weight. The dry samples were homogenized by powdering and 20 mg was extracted with 1 ml of 10% nitric acid for 24 h. The extract was used to determine the contents of Na⁺ and K⁺ using a flame atomic absorption spectrometer (AAS) (TAS-986, Beijing, China). Three replicates were performed for each treatment. One-way ANOVA followed by Tukey post hoc tests was used to test the differences among the control and treated samples. The differences were considered significant when $P < 0.05$. The same criteria of statistical analysis were applied for the following physiological measurements.

Measurement of H₂O₂ and malondialdehyde (MDA) accumulation

The H₂O₂ concentration in root was determined according to the KI reaction method (Ibrahim and Jaafar 2012). Fresh samples (0.1 g) were homogenized with 5 ml of 0.1% (w/v) trichloroacetic acid and centrifuged at 12,000g for 15 min. The reaction mixture consisted of 1 ml of 10 mM potassium phosphate buffers (pH 7.0), 2 ml of 1 M KI and 1 ml of the extracted supernatant. The absorbance at 390 nm was recorded. Five biological replicates of each treatment were used. One-way ANOVA was used to test the differences between the control and each treatment, followed by Tukey post hoc test. The differences were considered significant when $P < 0.05$.

To quantify MDA, fresh samples (0.1 g) were homogenized with 5 ml 0.1% (w/v) trichloroacetic acid and centrifuged at 3000g for 10 min. The mixture was incubated with 0.5 ml supernatant and 1.5 ml 0.67% thiobarbituric acid at 100 °C for 30 min and centrifuged at 3000g for 10 min. The absorbance of the supernatant at 450, 532 and 600 nm was recorded. The formula $C (\mu\text{M}) = 6.45 (\text{OD}_{532} - \text{OD}_{600})$

spectrop450 was used to calculate the MDA concentration (Draper and Hadley 1990). Five biological replicates of each treatment were used.

Transcriptomic analysis

RNA sample preparation, quantification and qualification

Total RNA extraction was performed from three biological replicates of *H. tuberosus* root tissues using Trizol (Invitrogen, Carlsbad, CA, USA) method, as described by the manufacturer with an additional chloroform extraction step. The RNA samples were solubilized in 50 μ l of diethyl pyrocarbonate (DEPC)-treated H₂O, and a 2 μ l aliquot was used for RNA quantification. The integrity and purity of the obtained RNA samples were first monitored by running agarose gel electrophoresis and NanoPhotometer[®] spectrophotometer (Implen, Westlake Village, CA, USA), and then assessed using the RNA Nano 6000 Assay Kit of the Agilent Bioanalyzer 2100 system (Agilent Technologies, Santa Clara, CA, USA). Quantification was carried out using a Qubit[®] RNA Assay Kit with a Qubit[®] 2.0 Fluorometer (Life Technologies, Carlsbad, CA, USA).

cDNA library preparation and Illumina HiSeq sequencing

A total amount of 1.5 μ g RNA per sample was used for sequencing library preparations with the NEBNext[®] Ultra[™] RNA Library Prep Kit for Illumina[®] (NEB, Ipswich, MA, USA) following the manufacturer's recommendations, and index codes were added to attribute sequences to each sample (Kumar et al. 2012). The PCR products were purified (AMPure XP system) and library quality was assessed on the Agilent Bioanalyzer 2100 system (Agilent Technologies). The clustering of the index-coded samples was performed on a cBot Cluster Generation System using the TruSeq PE Cluster Kit v3-cBot-HS following the manufacturer's instructions. Finally, samples were sequenced on a single lane of an Illumina HiSeq 4000 platform and 150 bp paired-end reads were generated.

Preprocessing of Illumina reads

Raw reads of FASTQ format were firstly processed through in-house Perl scripts to get high-quality clean reads. Reads containing adapter, ploy-N and reads of low quality (the percent of bases with Phred quality score ≤ 20 more than 50% of the reads) were removed. Next, Q20, Q30, GC-content and sequence duplication level of the obtained clean reads were calculated. All the downstream analysis was based on clean reads with high quality.

De novo transcriptome assembly

The Trinity software package (version 2.1.0) was used for de novo assembly of high-quality reads according to the previously described method (Grabherr et al. 2011). The left files (read1 files) from all libraries were pooled into one big left.fq file, and right files (read2 files) into one big right.fq file. The left.fq and right.fq were used for transcriptome assembly with the default settings for all parameters except min_kmer_cov, which was set to be 2.

Gene functional annotation

Assembled transcripts were BLAST searched against the NCBI non-redundant protein sequences database (Nr) and nucleotide sequences (Nt) using BLASTX with an e-value threshold of $1e-5$. The unigenes were also annotated using HMMER 3.0 package in Protein Family (Pfam) with hmmscan *e* value of 0.01. Based on the annotation output from blast Nr and Pfam, Gene Ontology (GO) analysis was performed by Blast2GO v2.5 (Götz et al. 2008), and the e-value filter for GO annotation was $1e-6$. In addition, gene functional annotation was conducted in the following databases: the manually annotated and curated protein sequence database (Swiss-Prot), Eukaryotic Ortholog Groups (KOG) and Clusters of Orthologous Groups of proteins (COG), Kyoto Encyclopedia of Genes and Genomes (KEGG) with an e-value threshold of $1e-10$.

Quantification of gene expression levels and differential expression analysis

To estimate the expression abundance of transcripts, RNA-seq by expectation maximization (RSEM) was used for FPKM (fragments per kilobase per transcript per million mapped reads) level measurement on each sample separately based on the mapping of RNA-seq reads to the assembled transcriptome (Trapnell et al. 2010; Li and Dewey 2011). Clean reads from different samples were mapped back individually onto the final transcriptome using the default RSEM parameters, and read count for each gene was obtained from the mapping results.

Differential expression analysis between control and salt-treated *H. tuberosus* plants was carried out using the DESeq R package (1.10.1) (Anders and Huber 2010). DESeq provide statistical routines for determining differential expression in digital gene expression data using a model based on the negative binomial distribution. The resulting *P* values were adjusted using the Benjamini and Hochberg's approach for controlling the false discovery

rate. Genes with an adjusted P value < 0.05 were considered as differentially expressed.

GO term and KEGG pathway enrichment analysis

GO enrichment analysis of the differentially expressed genes (DEGs) was implemented by the Goseq R packages based Wallenius non-central hyper-geometric distribution (Young et al. 2010), which can adjust for gene length bias in DEGs. TopGO was used to identify enriched GO terms. KOBAS (Mao et al. 2005) software was used to test the statistical enrichment of differential expression genes in KEGG pathways.

RT-PCR analysis

To validate the transcriptomic data, 11 DEGs were chosen for RT-PCR analysis. Total RNA was extracted with Trizol reagent (Invitrogen) from root tissues of control and 150 mM NaCl-treated *H. tuberosus*. RNA samples treated with RNase-free DNase I (TaKaRa, Tokyo, Japan) to remove genomic DNA. 10 μg of RNA was used for reverse transcription with PrimeScript™ RT reagent Kit (Perfect Real Time) (TaKaRa) according to the manufacturer's instructions and the cDNAs were used for RT-PCR analysis with specific primers. Quantitative RT-PCR was performed with the Applied Biosystems 7500 real-time PCR system using Power SYBR green chemistry (TaKaRa). Actin was quantified as an internal control and the $2^{-\Delta\Delta C_t}$ method was used to analyze the differential expression (Livak and Schmittgen 2001). The mean of three biological replicates, for which three technical replicates were averaged, was presented. Genes were considered to be differentially expressed if (1) fold change ≥ 1.5 or ≤ 0.6 (2) P value from post hoc ANOVA test ≤ 0.05 .

Proteomic analysis

Protein extraction

Approximately, 5 g of root samples was ground in liquid nitrogen into a fine powder, which was then suspended in 25 ml of ice-cold acetone containing 10% trichloroacetic acid and 65 mM DTT. After incubation at $-20\text{ }^\circ\text{C}$ for 4 h, the suspension was centrifuged at 6000 g for 45 min at $4\text{ }^\circ\text{C}$ to collect the pellets. The resulting pellet was washed twice with cold acetone. After air drying, the pellet was dissolved in 30 times the volume of (m/v) the lysis buffer (pH 7.6) containing 4% SDS, 100 mM Tris-HCl and 1 mM DTT. The samples were sonicated and boiled at $100\text{ }^\circ\text{C}$ for 30 min, followed by centrifugation at 14,000 g for 45 min at $25\text{ }^\circ\text{C}$. The supernatant was collected as a protein extract. Protein

assays were performed with EZQ Protein Quantitation Kit (Invitrogen).

Protein digestion and iTRAQ labeling

100 μg protein from each sample was digested into peptides with trypsin (Promega, Madison, WI, USA). Peptides were subsequently cleaned up with C18 desalting columns (The Nest Group Inc., Southborough, MA, USA) and then lyophilized to dryness. iTRAQ labeling was performed according to the manufacturer's instructions for the iTRAQ reagents 8-plex kit (AB Sciex Inc., Framingham, MA, USA). The control biological replicate samples were labeled with iTRAQ tags 117 and 118, and the salt-treated biological replicate samples labeled with tags 119 and 121, respectively.

After labeling, the samples were combined together and lyophilized. The peptide mixtures were dissolved in strong cation exchange (SCX) solvent A (25% (v/v) acetonitrile, 10 mM ammonium formate and 0.1% (v/v) formic acid, pH 2.8). The peptides were fractionated on Ultremex SCX column ($4.6 \times 250\text{ mm}$) using Shimadzu LC-20AB HPLC at a flow rate of 0.2 ml min^{-1} . The subsequent experiment was performed as described in Pang et al. (2010). The eluted peptides were pooled into 16 fractions for LC-MS/MS analysis, desalted with a Strata XC18 column (Phenomenex, Torrance, CA, USA) and vacuum dried.

LC-ESI-MS/MS analysis by Q Exactive

Each fraction was dissolved in Solvent A (5% ACN, 0.1% formic acid) and centrifuged at 20,000 g for 10 min. In each fraction, the final concentration of peptide was approximately $0.5\text{ }\mu\text{g }\mu\text{l}^{-1}$ on average. Then, 8 μl of supernatant was loaded onto a Shimadzu LC-20 AD nanoHPLC by the autosampler onto a C18 trap column, and the peptides were eluted onto an analytical C18 column (inner diameter 75 μm) that was packed in-house. Peptides were eluted using a gradient of 5–80% (v/v) acetonitrile in 0.1% formic acid 65 min at a flow rate of 300 nl min^{-1} combined with a Q Exactive mass spectrometer (Thermo Fisher Scientific, Waltham, MA, USA). Briefly, the mass spectrometer was operated in positive ion mode, and MS spectra were acquired over a range of 350–2000 m/z . The resolving powers of the MS scan and MS/MS scan were set as 70,000 and 17,500, respectively. The top ten most intense signals in the acquired MS spectra were selected for further MS/MS analysis, with isolation width at 2 Da. Peptides were selected for MS/MS using a high-energy collision dissociation operating mode with a normalized collision energy setting of 28.0. The automatic gain control (AGC) target values for both scans were set to $3e^6$. The maximum injection times (IT) for the survey scan and HCD scan were 50 and 100 ms, respectively.

Dynamic exclusion was set to 15 s and the underfill ratio was defined as 1%.

Sequence database search and data analysis

The raw data were processed by Proteome Discoverer 2.1.1.21 (Thermo Fisher Scientific). The processing workflow used SEQUESTHT algorithm to search against the Green plants non-redundant database (351,289 entries) with the following parameters: 10 ppm for MS1 tolerance, 0.5 Da for MS2 tolerance, trypsin for the enzyme and 2 as the maximum missed cleavage allowed. We also searched against our unigene library built from de novo assembly sequencing transcriptomic. The consensus workflow set the false discovery rates (FDR) at both peptide and protein levels to be 1%. At least one unique peptide with 99% confidence was used for protein identification. The redundant proteins were automatically grouped into protein groups using the SEQUESTHT.

The protein abundance for each iTRAQ quantification channel was exported and further analysis was performed using the R statistical software (version 3.2.3) as described previously with modifications (Zhang et al. 2016). Briefly, the abundance of each protein group was aggregated by summing the abundance of the constituent proteins. Subsequently, the data were normalized by the total abundance

of each quantification channel. The correlation of iTRAQ-based protein quantification among replicates was performed using Spearman’s non-parametric method. The proteins with $0.85 \geq \text{fold change} \geq 1.2$ were defined as being significantly differentially expressed. The Student’s *t* test was used to calculate the *P* value at a significance level of 0.05. Protein functional classification of all the differentially expressed proteins identified by iTRAQ was performed by GO and KEGG pathway analyses.

Results

Effects of salt stress on plant growth

Plant growth and development are strongly inhibited by salt stress. For example, significant reduction in plant size and remarkable chlorosis have been observed in the model plant *Arabidopsis thaliana* under 150 mM NaCl treatment for 2 weeks (You et al. 2016). In contrast, *H. tuberosus* plants treated with different levels of NaCl did not show apparent chlorosis. However, a NaCl concentration-dependent reduction in the overall plant status was observed with 250 mM NaCl showing a drastic effect (Fig. 1a). Sprout and root elongation was slightly inhibited under 50 and 150 mM NaCl

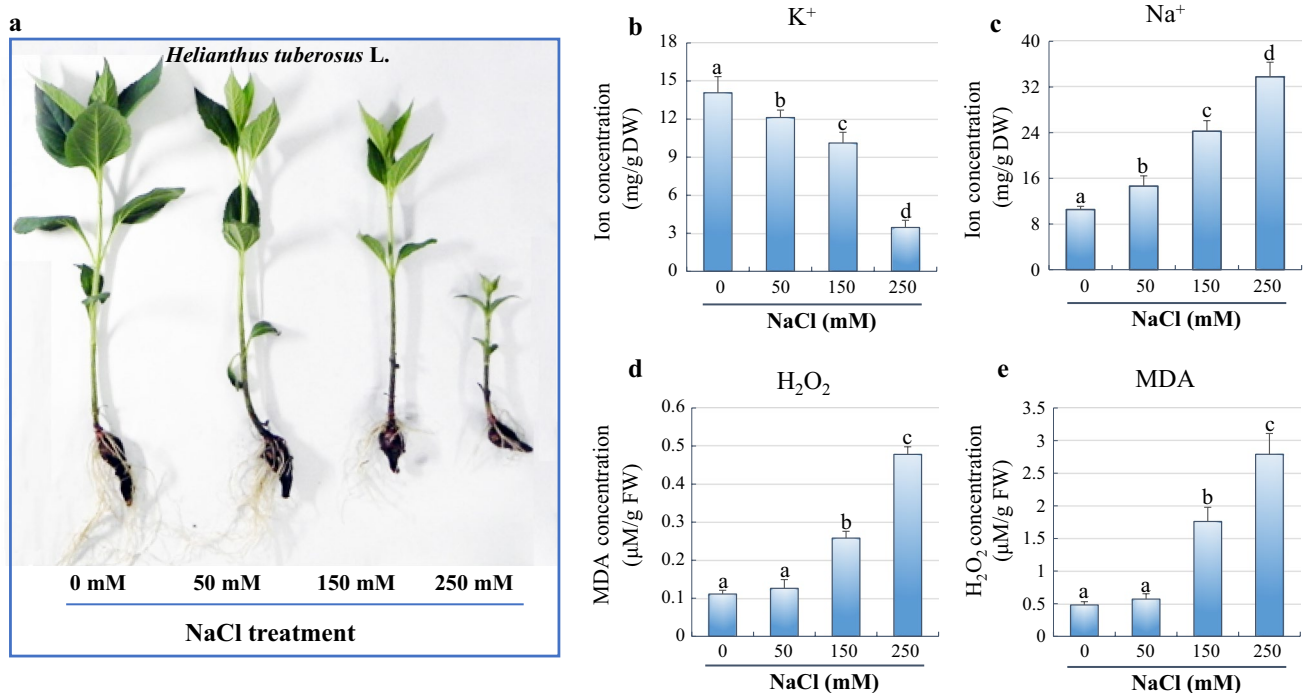


Fig. 1 Effects of NaCl treatment on *H. tuberosus* growth. **a** Growth phenotype of *H. tuberosus* under control and stress conditions. After exposure for 15 days, **b** K⁺ and **c** Na⁺ content, **d** H₂O₂ and **e** MDA

accumulation from each group were measured. Error bars show the SE for biological replicates. Significant differences (*P* < 0.05 by one-way ANOVA analysis) are indicated by asterisk

Table 1 Effect of NaCl treatment on the growth of *H. tuberosus*

Parameters	NaCl concentration (mM)			
	0	50	150	250
Sprout length (cm)	23.22 ± 0.47a	21.60 ± 0.35b	18.30 ± 0.34c	8.02 ± 0.57d
Root length (cm)	8.27 ± 0.64a	7.83 ± 0.62a	5.47 ± 0.52b	2.75 ± 0.21c

Data represent mean ± SD for biological replicates ($n = 15$). Significant differences are indicated by different letters ($P < 0.05$ by one-way ANOVA analysis)

treatment and the growth was significantly reduced after 250 mM NaCl stress compared to the control (Table 1).

The contents of Na^+ and K^+ were measured to analyze the impact of salt stress on ion homeostasis in *H. tuberosus*. The results showed that the K^+ content was significantly lower in the NaCl-treated roots than in the controls (Fig. 1b). By contrast, the Na^+ content showed significant increase under NaCl stress (Fig. 1c). These data suggest that there was a high salt ion accumulation in the root of *H. tuberosus* and an outflow of K^+ was caused by salt stress. Supporting previous findings declared that a lower K^+ content and a higher Na^+/K^+ ratio were detected in plants when it was stressed by salt treatment (Sun et al. 2015). In addition, salt stress reprograms the balance between the generation and scavenging of ROS (Abogadallah 2010). In agreement with that, plants accumulated higher concentration of H_2O_2 and MDA under 150 and 250 mM NaCl treatment, but not 50 mM NaCl (Fig. 1d, e), indicating that the oxidative bursts were activated by relatively higher salt stress in *H. tuberosus*. Based on phenotype observation and physiological investigation, to get relatively healthy plants that display salt-resistant phenotype, we chose 150 mM NaCl-treated plants for the transcriptomic and proteomic analysis.

De novo assembly and quality assessment of transcriptome

To generate an overview of transcriptome with sufficient depth coverage for differential gene expression analysis in *H. tuberosus*, Illumina short-read sequencing and de novo transcriptome assembly were conducted on a HiSeq 4000 platform. RNA-seq library was prepared from root tissue of *H. tuberosus*. The details of the total number of reads obtained under control and stress conditions are listed in Table 1. In summary, a total of 62,105,592 paired-end reads (150 bp) were obtained with sequencing error rates less than 2%. Preprocessing of the raw reads was performed by removing reads containing adapter/primer sequences, reads with indeterminate bases ratio beyond 10%, reads of low-quality sequences and duplications. A total of 60,069,922 clean reads (more than 96% of all raw reads) were obtained for transcriptome assembly (Table 2). The resultant *H. tuberosus* transcriptome contains 293,823 transcripts ranging from 201 to 1500 bp (Table 3). A total of 190,567 unigenes were

Table 2 Sequencing statistics for *H. tuberosus*

Sample	Raw reads	Clean reads	Error rate (%)	Q20 (%)	GC (%)
Control 1	52777502	49765032	0.02	96.29	44.80
Control 2	53878338	51845050	0.02	96.62	44.88
Control 3	60071828	57161302	0.02	96.08	44.98
Treat 1	60842170	58534126	0.02	96.70	44.93
Treat 2	59454444	57660866	0.01	97.33	44.14
Treat 3	62105592	60069922	0.02	97.13	44.39

identified. The details of length interval and size distribution of transcripts and unigenes are shown in Table 3 and Fig. 2.

Transcriptome annotation

To gain exhaustive gene function information, the assembled transcripts were BLAST searched against seven databases: Nr, Nt, Pfam, GO, KOG/COG, Swiss-Prot, KEGG and GO, resulting in the annotation of 80,511 unigenes (42.24% of all the assembled transcripts) with an E-value threshold of $1e-5$ based on the length of query sequence and hit score (Suppl. Table S1 and S2). The detailed information of plant species similarity, e-value distribution and sequence similarity distribution of assembled transcripts which were analyzed by Blast Nr is displayed in Suppl. Fig. S1. Five representative databases were chosen to illustrate the number of overlapped genes which were successfully annotated by these databases tools. As the venn diagram shows, all the annotation tools output a total of 9,424 unigenes from *H. tuberosus* transcriptome (Suppl. Fig. S2).

Annotated transcripts were further categorized into GO terms and KEGG pathways. For GO analysis, the transcripts were annotated into biological process (GO:0008150), cellular component (GO:0005575) categories, and molecular function (GO:0003674). 56 terms of GO classification were annotated from expressed 47,066 unigenes (Fig. 3, Suppl. Table S3). Overall and multilevel GO distribution within these broad GO categories is shown in Fig. 3. As shown, most annotated unigenes in the biological process were involved in cellular process (GO:0009987), metabolic process (GO:0008152), single-organism process (GO:0044699) and biological regulation (GO:0065007). According to

Table 3 Assembly statistics for *H. tuberosus*

Parameter	Mean length (bp)	Min length (bp)	Median length (bp)	Max length (bp)	N50 (bp)	N90 (bp)	Total nucleotides	Numbers
Transcripts	624	201	377	14,609	907	261	183,237,654	293,823
Unigenes	533	201	318	14,609	709	239	101,487,178	190,567

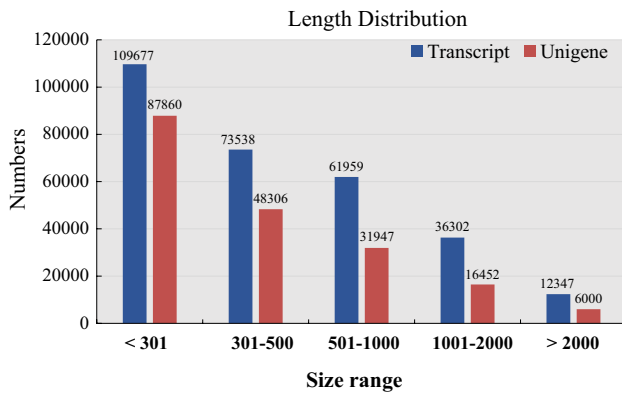


Fig. 2 Transcript length distribution. Transcript and unigene size distribution of *H. tuberosus* transcriptome and the total number of assembled transcripts and unigenes are indicated in the diagram

the category of molecular function, the highest portion of annotated unigenes was enriched in terms of binding (GO:0005488) and catalytic activity (GO:0003824) (Fig. 3, Suppl. Table S4). We have also classified transcripts among KEGG pathways; 19 pathways were assorted based on five

branches including cellular processes, environmental information processing, genetic information processing, metabolism and organismal system (Fig. 4, Suppl. Table S5). On the basis of KEGG analysis, most unigenes were annotated into sub-branches of carbohydrate metabolism, translation and folding, sorting and degradation.

Differentially expressed transcript

To generate resource of differentially expressed genes associated with salt tolerance of *H. tuberosus*, three independent biological replicates for transcriptomics analysis of each group were produced to analyze the gene expression changes under control and salt stress conditions. Comparative analysis for identification of salt-responsive genes was performed using the DESeq R package (1.10.1) (Anders and Huber 2010). Transcripts with an adjusted *P* value < 0.05 found by DESeq were assigned as differentially expressed. A total of 77,320 transcripts were expressed in both control and stressed samples (Fig. 5a, Suppl. Table S6), and 2165 and 3267 transcripts were shared among up-regulated and down-regulated transcripts (Fig. 5b, Suppl. Table S7 and S8).

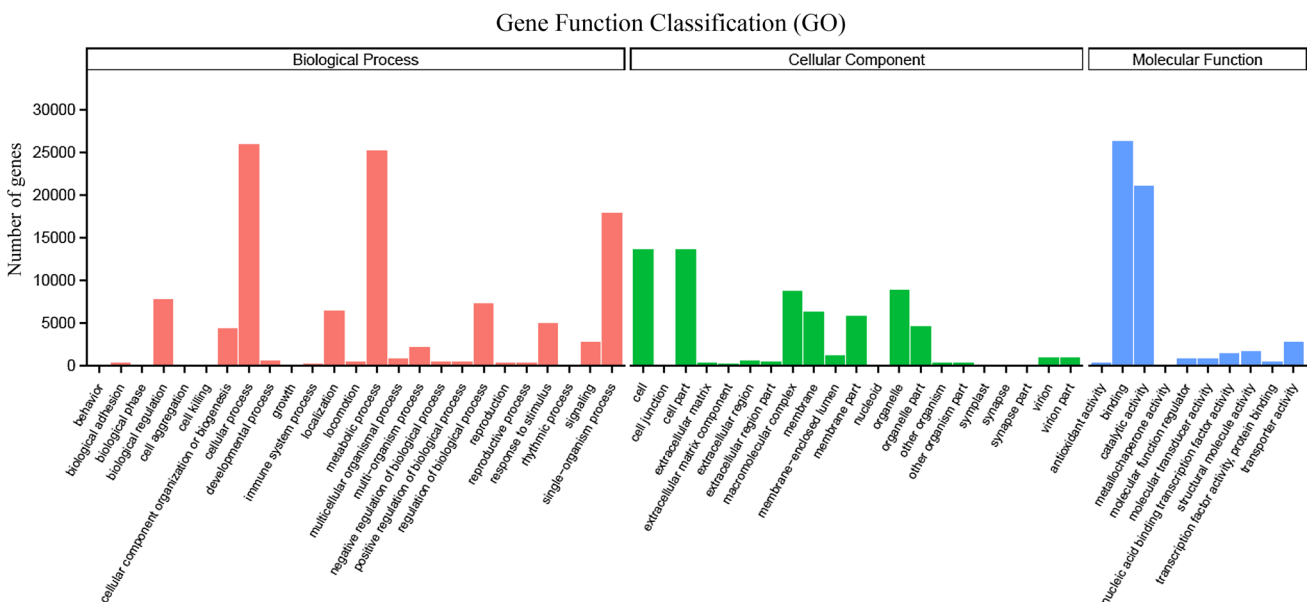


Fig. 3 GO categorization of all annotated unigenes identified from *H. tuberosus* transcriptome. Go analysis for gene functional classification shows the number of genes involved in the biological process, cellular component and molecular function, respectively

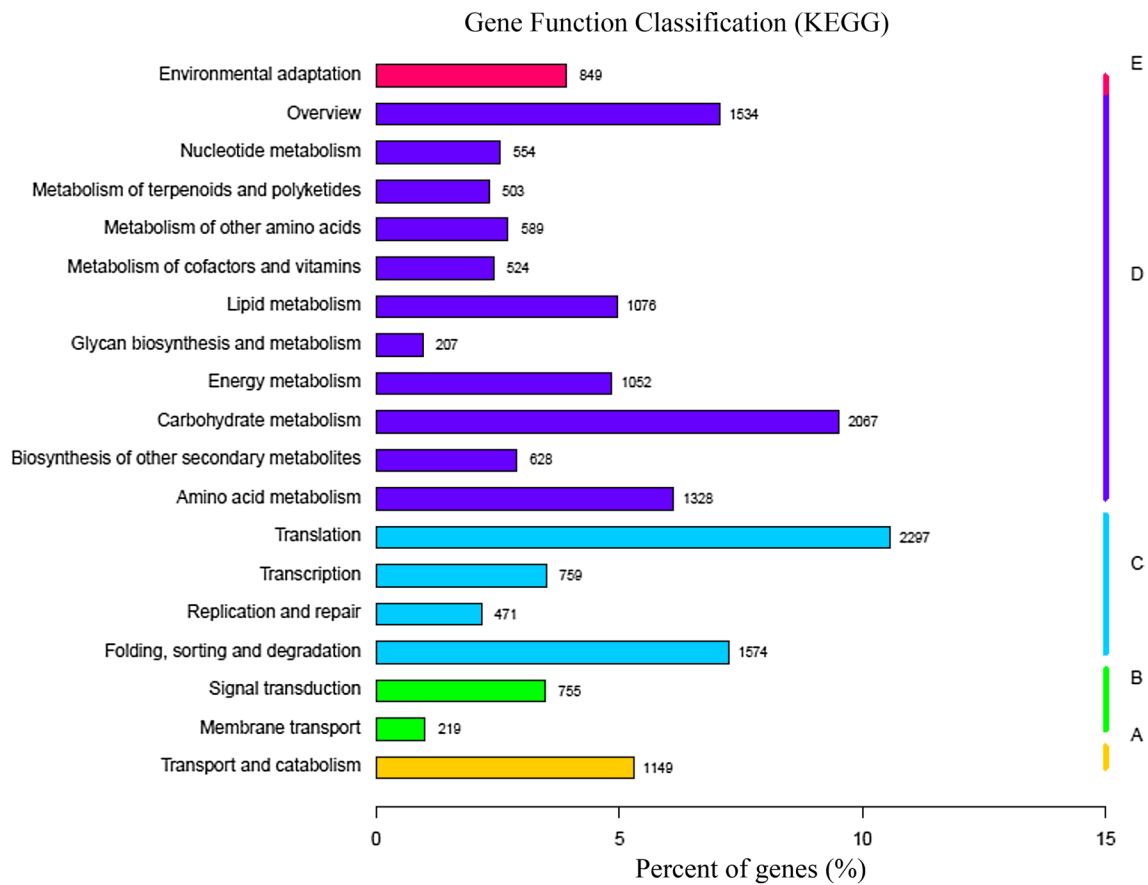


Fig. 4 KEGG pathway analysis of all annotated unigenes identified from *H. tuberosus* transcriptome. Five branches were assorted based on KEGG enrichment including *A* cellular processes, *B* environ-

mental information processing, *C* genetic information processing, *D* metabolism and *E* organismal system. The number of genes involved in each pathway was marked

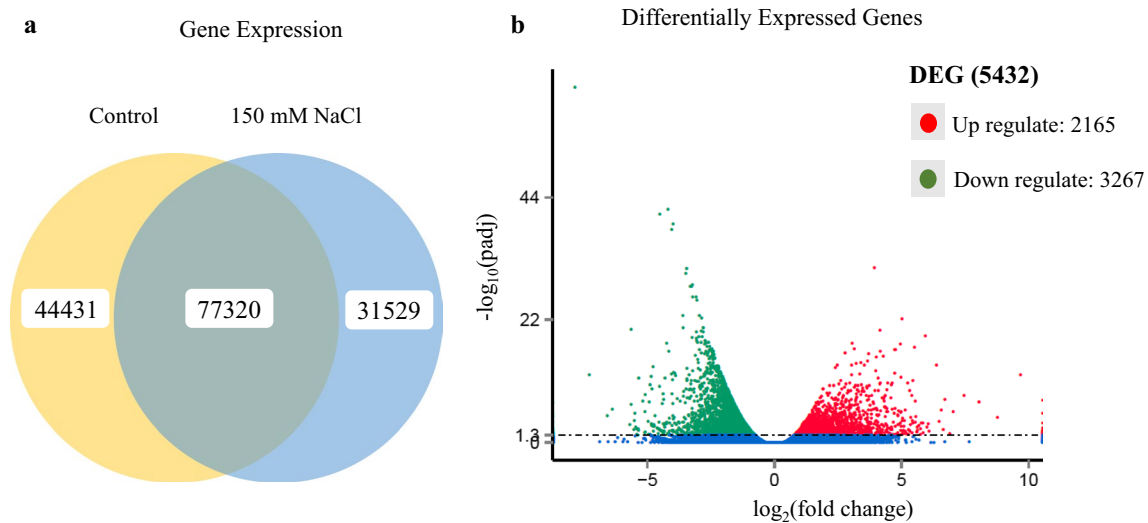


Fig. 5 Gene expression in control and salt-treated *H. tuberosus*. **a** Venn diagram showing the numbers of genes expressed differentially under control and 150 mM NaCl-stressed plants. **b** Volcano plot of

differentially expressed transcripts in *H. tuberosus* with stress treatment at $P_{adj} < 0.05$; the up-regulated and down-regulated genes are represented by green and red dots, respectively

GO and KEGG pathway enrichment analysis

To understand the functions of DEGs, all the genes were mapped into terms in the GO database (Suppl. Table S9 and S10). Then the most significantly enriched GO term response to salt stress compared to the reference gene background was analyzed by Goseq (Young et al. 2010) based on Wallenius non-central hyper-geometric distribution. According to the biological process, the up-regulated DEGs that mapped to organonitrogen compound biosynthetic process, cellular nitrogen compound biosynthetic process (GO:0044271) and single-organism metabolic process (GO:0044710) constituted a high proportion during NaCl treatment (Fig. 6a, Suppl. Table S11). Three terms of oxidoreductase activity (GO:0016491), structural constituent

of ribosome (GO:0003735) and structural molecule activity (GO:0005198) occupied the highest part in molecular function (Fig. 6a, Suppl. Table S11). Furthermore, most of these up-regulated DEGs accumulated in the cell part (GO:0044464) and intracellular part (GO:0005622) based on cellular component annotation (Fig. 6a). With regard to down-regulated DEGs, most of them were enriched in metabolic process (GO:0008152) under biosynthetic process category, and the most represented GO term of down-regulated DEGs under salt stress was transcription factor complex (GO:0005667) based on cellular component category (Fig. 6b, Suppl. Table S12). Of the down-regulated genes which were classified into molecular function, most of them belonged to the terms of ion binding (GO:0043167), transferase activity (GO:0016740), phosphorylation

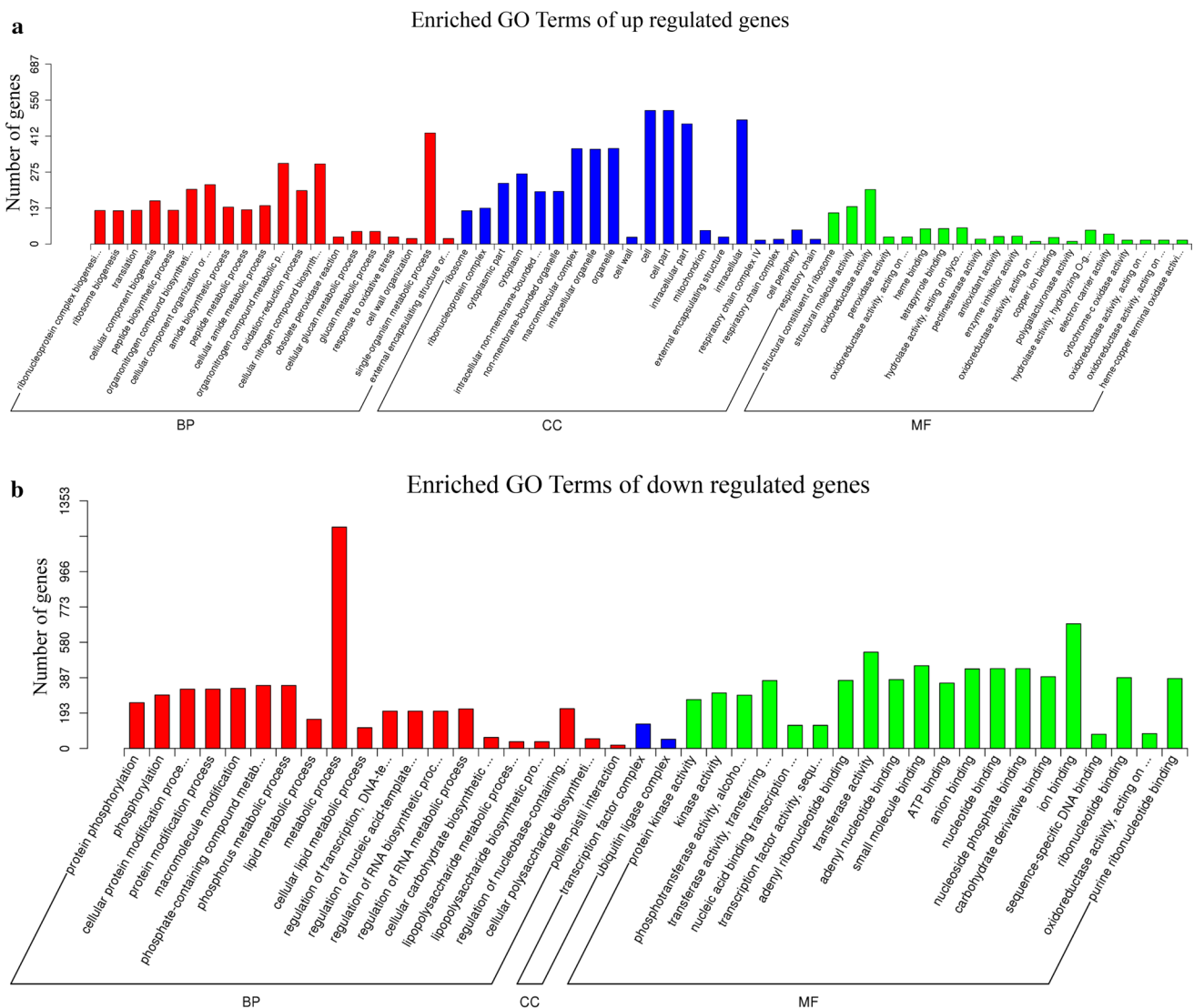


Fig. 6 GO terms enrichment of differentially expressed transcripts. Number of genes **a** up-regulated and **b** down-regulated in *H. tuberosus* under 150 mM NaCl stress at associated enriched GO terms

(GO:0016310) and catalytic activity (GO:0003824) (Fig. 6b, Suppl. Table S12).

RT-PCR analysis of gene expression

To further verify the results from the RNA-Seq work, 11 transcripts of each tissue were selected for quantitative RT-PCR analysis (Suppl. Table S13). The ID of these genes are as follows: c130738_g2 (peroxidase 5-like), c131209_g1 (alkaline leaf peroxidase), c117640_g1 (monodehydroascorbate reductase), c142572_g1 (F-type H⁺-transporting ATPase subunit beta), c113756_g1 (auxin-responsive family protein), c142483_g1 (respiratory burst oxidase homolog protein C), c141004_g1 (potassium transporter 1), c130593_g1 (chloride channel protein CLC-f), c120523_g1 (transcription factor ILR3), c143610_g1 (probable LRR receptor-like serine/threonine-protein kinase) and c131342_g3 (abscisic acid receptor PYL4), which were identified to be differentially expressed in *H. tuberosus* transcriptome under salt stress. The results of RT-PCR analysis are shown in Fig. 7. Except one gene c117640_g, the expression trends of all the unigenes from the qRT-PCR were consistent with the RNA sequencing analysis (Fig. 7). These results demonstrate that the transcriptomic profiling data accurately reflected the response of *H. tuberosus* to salt stress.

Comparative proteome analysis

To better dissect the molecular modified network in *H. tuberosus* response to salt stress, we utilized iTRAQ labeling strategy to perform a quantitative proteomics and analyze the global protein changes in salt-treated plants based on de novo assembly transcriptomic analysis. A fine correlation

of iTRAQ quantification has been shown between two biological replications from the control and salt-treated groups (Suppl. Fig. S3). 1,843 proteins were quantified from approximately 50,000 peptides (Suppl. Table S14). Among these proteins, 43 differentially expressed proteins were identified during salt condition treatment (Suppl. Fig. S4). 19 of them were up-regulated and 24 proteins down-regulated by salt stress in *H. tuberosus* (Table 4). GO enrichment was set to analyze the key cellular process affected by salt stress. Under the category of biological process, the majority of the differentially expressed proteins were classified into metabolic process, response to stimulus and regulation of biological process (Fig. 8a). These proteins were mainly involved in catalytic activity and nucleotide binding depending on molecular function category (Fig. 8a). KEGG analysis revealed that the corresponding pathways were translation, environmental information processing, energy metabolism, starch and sucrose metabolism, stress, defense, etc. (Fig. 8b).

Indeed, as integrated comparative transcriptomic and proteomic data showed, several cellular processes such as metabolic process and ribosome activity were impacted by changing key regulators at both transcript and protein level in *H. tuberosus* under salt stress.

Discussion

Previous studies had provided valuable genetic information such as a de novo transcriptome and an EST database from the Compositae Genome Project database for *H. tuberosus* (Barker et al. 2008; Jung et al. 2014). However, resource to explore stress-related molecular mechanism in *H. tuberosus*

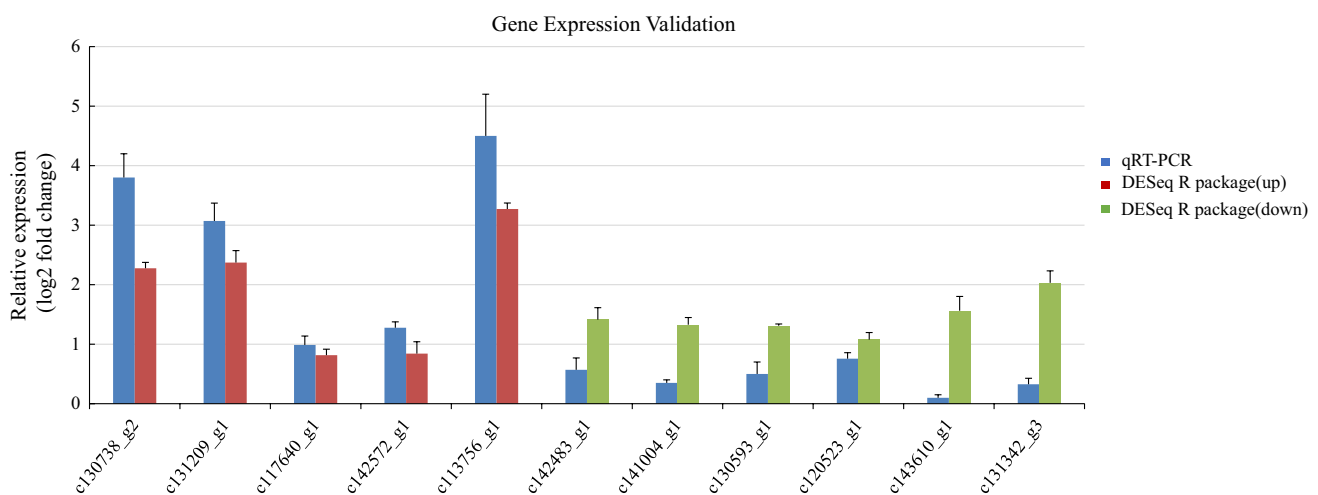


Fig. 7 Quantitative RT-PCR validation analysis of gene expression of salt-responsive transcripts in *H. tuberosus* root tissues. Actin was quantified as an internal control and the $2^{-\Delta\Delta C_t}$ method was used to

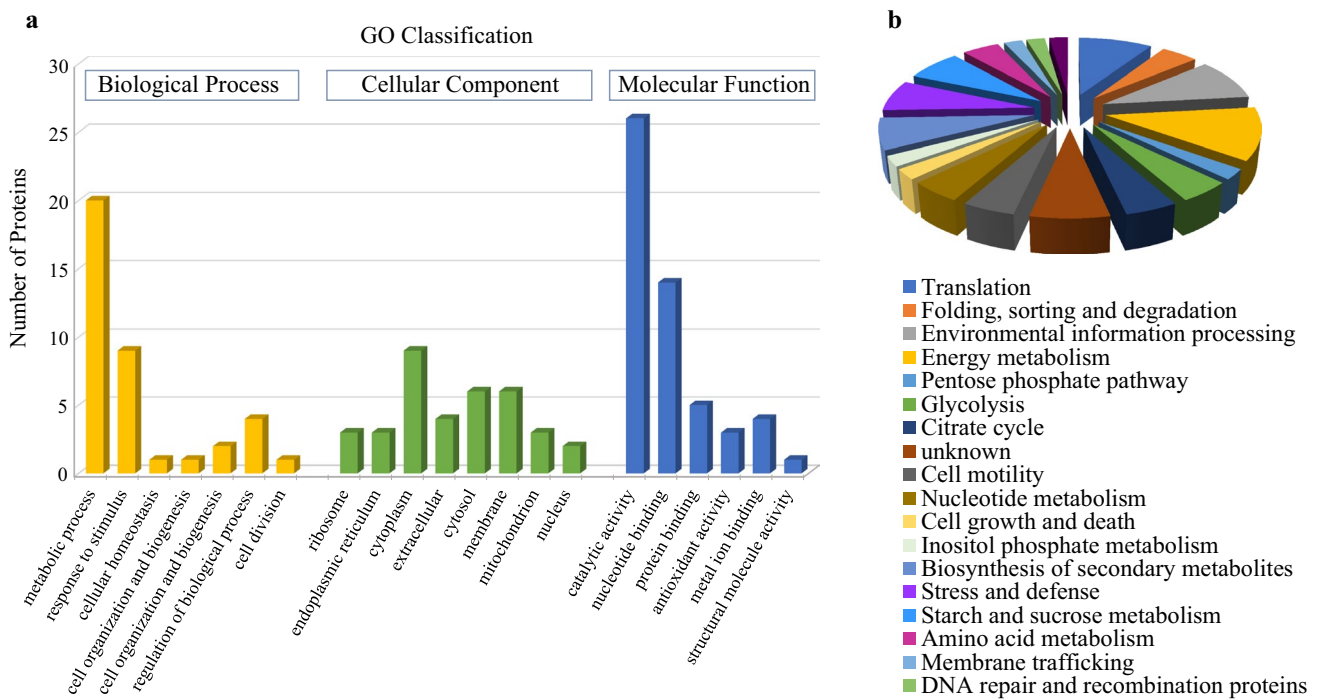
analyze the differential expression. The experiments were repeated three times. Each data point represents mean \pm SE ($n = 3$)

Table 4 Proteomics responses to salt stress in *H. tuberosus*

Spot No.	Protein name	Protein abundance		Fold change	P-Value	M_w (kDa)	Calc. pI
		Control_mean	Treat_mean				
Translation							
41	60S ribosomal protein L10A, partial	77.75	98.75	1.27	0.03	8.7	9.79
85	40S ribosomal protein S8	14,148.98	17,347.24	1.23	0.03	24.5	10.5
188	60S ribosomal protein L30	2763.94	2206.54	0.80	0.04	12.4	9.58
2312	Translation initiation factor 3 subunit B	412.59	530.59	1.29	0.02	82.6	5.2
Folding, sorting and degradation							
405	Protein disulfide-isomerase-like	3653.34	2756.49	0.75	0.05	55.4	5.4
Environmental information processing							
710	Dynammin-related protein 1B isoform X1	96.00	132.20	1.38	0.03	68.1	7.77
1142	Calcium-transporting ATPase 4, endoplasmic reticulum-type	1934.63	2458.62	1.27	0.00	116.5	5.45
1250	Chaperonin 20 isoform 2	4303.97	3390.62	0.79	0.05	26.8	8.62
Energy metabolism							
547	ATPase, AAA-type, CDC48 protein	5016.19	6509.74	1.30	0.02	90.3	5.16
974	Thiosulfate/3-mercaptopyruvate sulfurtransferase 1	351.54	278.12	0.79	0.01	16.1	5.47
1429	Pyruvate orthophosphate dikinase	200.40	148.56	0.74	0.01	95.3	5.52
1976	NAD(P)-linked oxidoreductase superfamily protein	2237.95	3129.35	1.40	0.03	37.8	6.3
Citrate cycle							
2174	Pyruvate phosphate dikinase 2	265.47	194.41	0.73	0.02	107.3	5.76
2535	2-oxoglutarate dehydrogenase, E1 component	144.98	118.44	0.82	0.05	116.3	7.3
2545	Chaperone protein htpG family protein	1018.58	1489.66	1.46	0.04	88.2	5.01
Glycolysis							
114	Glyceraldehyde-3-phosphate dehydrogenase, partial	593.12	481.02	0.81	0.03	35.1	6.89
629	2-Oxoglutarate (2OG) and Fe(II)-dependent oxygenase	151.47	243.56	1.61	0.01	36.4	6.1
1064	Triosephosphate isomerase, cytosolic	7054.07	5264.40	0.75	0.03	27.1	6.21
Pentose phosphate pathway							
1301	UDP-glucose dehydrogenase	136.44	164.42	1.21	0.03	52.9	6.13
Starch and sucrose metabolism							
651	Xyloglucan endotransglucosylase/hydrolase protein 23	2006.77	1335.41	0.67	0.01	31.7	7.2
1009	Glycosyl hydrolase family protein	412.77	274.54	0.67	0.01	66.3	5.35
2082	Glucan endo-1,3-beta-glucosidase 7, partial	1038.78	841.74	0.81	0.03	60.2	7.3
2668	Xyloglucan endotransglucosylase/hydrolase protein 8	517.17	426.84	0.83	0.04	34.4	4.84
Amino acid metabolism							
1922	Aspartate aminotransferase, chloroplastic-like	539.85	424.69	0.79	0.02	49.9	9.1
2158	Cystathionine beta-synthase (CBS) family protein isoform 1	1848.08	1366.10	0.74	0.02	22.7	8.94
Nucleotide metabolism							
123	FAD-binding and BBE domain-containing protein	4404.62	3534.17	0.80	0.04	59.8	9.26
709	FAD-binding Berberine family protein	5114.49	3350.25	0.66	0.03	60.3	9.67
Inositol phosphate metabolism							
912	Inositol-3-phosphate synthase	1292.35	1037.08	0.80	0.02	56.2	5.94
Biosynthesis of secondary metabolites							
66	10-Hydroxygeraniol dehydrogenase	1535.36	3639.16	2.37	0.02	38.9	7.11
840	Tetrahydrocannabinolic acid synthase-like	220,665.50	115,230.68	0.52	0.04	60.5	9.42
1995	Pectin acetyltransferase 8-like isoform X1	692.56	270.97	0.39	0.05	43.9	8.51
Cell motility							
546	Villin-3-like	1508.21	2085.01	1.38	0.00	107.9	6.15
1782	Villin-3-like	176.04	127.92	0.73	0.03	106.5	6.06

Table 4 (continued)

Spot No.	Protein name	Protein abundance		Fold change	P-Value	M_w (kDa)	Calc. pI
		Control_mean	Treat_mean				
Cell growth and death							
798	ATP-dependent Clp protease	2596.57	3257.97	1.25	0.02	71.5	8.66
Stress and defense							
261	Peroxidase 5-like	4926.61	2796.39	0.57	0.00	28.8	8.16
541	Peroxidase 50-like	443.23	330.24	0.75	0.01	35.9	9.35
2264	Catalase, partial	602.11	812.76	1.35	0.04	54.9	7.09
Membrane trafficking							
2147	Coatomer, alpha subunit	29.94	41.40	1.38	0.04	137.1	7.01
Vesicle trafficking							
768	Alpha-soluble NSF attachment protein 2	226.14	300.69	1.33	0.01	27.2	5.33
DNA repair and recombination proteins							
2090	AP-5 complex subunit beta	88.10	110.13	1.25	0.03	124.3	6.18
Unknown							
1780	TO68-13, partial	22,482.25	18,198.20	0.81	0.04	10.8	4.93
1911	Predicted protein	953.77	1208.02	1.27	0.02	90.5	5.24
2041	TUDOR-SN protein 1	198.66	244.84	1.23	0.01	110	7.5

**Fig. 8** Functional classification of differentially expressed proteins identified in *H. tuberosus* under salt stress. **a** GO terms enrichment of differentially expressed proteins. **b** Protein categories from KEGG analysis

remained limited. In this work, we performed deep sequencing analysis and de novo transcriptome assembly of *H. tuberosus* using the Illumina HiSeq 4000 platform. The high number of sequenced reads resulted in significant coverage of the transcriptome, allowing gene characterization

and quantification of transcripts in control and salt-treated plants. Thus, a comprehensive view of *H. tuberosus* response to salt stress at the transcriptomic level was established, and important genes and gene categories modulating salt tolerance were identified. Then, iTRAQ-labeled proteomics gave

further perspective on which key cellular processes undergo regulation under salt treatment.

Transcriptome assembly and annotation

It had been demonstrated that different sequencing platforms affect the following quantitative and qualitative gene expression analysis (de Sá et al. 2015). We obtained a total of 60,069,922 high-quality clean reads, which accounted for more than 96% of the raw reads. Compared to a ratio of 68.37% from a previous sequencing work on *H. tuberosus*, our significantly improved results showed the robust performance of the HiSeq 4000 platform (Jung et al. 2014). The de novo transcriptome assembly showed that 293,823 transcripts were identified in root with N50 of 907 and 201 bp minimum sequence length, of which 16.5% were longer than 1 kb. 80,511 transcripts were successfully annotated by multi-database; moreover, approximately 45% unigenes annotated to Blast Nr covered the matched protein sequences by more than 80%, which is comparable to many other de novo-assembled plant transcriptomes such as *Cuscuta pentagona*, *Oxytropis ochrocephala*, *Medicago falcata*, *Trifolium pratense* L. (Ranjan et al. 2014; Yates et al. 2014; Miao et al. 2015; He et al. 2015), enunciate satisfactory assembly and annotate quality.

On the basis of gene expression analysis, 2165 and 3267 transcripts were identified to be up-regulated and down-regulated in salt-treated *H. tuberosus* plants. A gene-regulatory library governing *H. tuberosus* response to salt stress was also built accordingly. In addition, the GO and KEGG pathway enrichment analysis revealed that the DEGs were overly represented in processes associated with nitrogen compound biosynthesis, single-organism metabolism, oxidoreductase activity, and ribosome and ion binding, which had been shown to play an important roles in salinity tolerance (Zhu 2001; Shabala et al. 2015; Park et al. 2016).

Metabolic process

This study showed the majority of DEGs related to the metabolic process in *H. tuberosus*. The correlated encoding proteins were mainly involved in cellular metabolic process such as nitrogen compound biosynthesis (616 DEGs, 306 up-regulated, 310 down-regulated) and organic substance metabolism (1725 DEGs, 727 up-regulated, 998 down-regulated). Particularly, 129 genes encoding key metabolic enzymes catalyzing carbohydrate metabolic process were significantly up-regulated by salt treatment. The quantitative proteomic result also displayed several enzymes involved in citrate cycle, glycolysis and pentose phosphate pathway having higher expression abundance in salt-treated plants, indicating that the carbohydrate metabolism was activated in *H. tuberosus* under salt stress.

Among the up-regulated genes, genes encoding xyloglucosyl transferase, alpha-glucosidase, beta-glucosidase and endoglucanase in the glucan metabolic pathway were remarkably induced by NaCl treatment. Glucan is a polysaccharide of D-glucose monomers linked by glycosidic bonds. Xyloglucosyl transferase catalyzes the breakdown of beta-(1,4) bond in the backbone of a xyloglucan (Thompson and Fry 2001), alpha- and beta-glucosidase are hydrolases that cleave the individual glucosyl residues from glucans into their monomers glucose (Lee et al. 2012; Baiya et al. 2014). As extrapolation, cleavage of glucan causes the accumulation of glucose monomers, which make plants adapt to a saline environment. In salt-resistant maize varieties, monosaccharides such as glucose and fructose were highly accumulated (Richter et al. 2015). Moreover, 15 starch-metabolic process-related genes encoding beta-xylosidase, glycosyl hydrolases, glucose-6-phosphate isomerase, polygalacturonase, sucrose-phosphate synthase and pectinesterase also showed higher expression levels in NaCl-treated plants. These findings suggested that the accumulation of monosaccharides might be increased by the enhancement of polysaccharide hydrolysis in *H. tuberosus* under salt stress. Soluble carbohydrates play a key role as osmolytes and energy resource in salt defense, which has been demonstrated to be especially important in halophyte species (Wang et al. 2013). The richness of carbohydrates such as glucan, inulin and starch in *H. tuberosus* is believed to function as soluble sugar reserves to cope with abiotic stress (Edelman and Jefford 1968). In our study, we observed a strong co-differentially expressed gene network to reprogram sugar profiles of *H. tuberosus* roots in response to salt stress. Similar expression patterns of sugar metabolic-related transcripts had also been observed in rice and potato under salt stress (Boriboonkaset et al. 2013; Asensi-Fabado et al. 2015), supporting the notion that accumulation of soluble sugar is a common mechanism.

Intriguingly, the expression of four genes involved in the trehalose biosynthetic process, alpha-trehalose-phosphate synthase and trehalose-phosphate phosphatase, were significantly inhibited by salt stress. Trehalose is a disaccharide composed of two glucose molecules (Higashiyama 2002). The trehalose metabolism has been implicated in sugar signaling, and enhanced trehalose metabolism positively regulates abiotic stress tolerance (Krasensky et al. 2014). For example, the transcripts of trehalose pathway genes were elevated in salt-treated maize and overexpression of the trehalose-6-phosphate phosphatase gene *OsTPPI* confers stress tolerance in rice (Ge et al. 2008; Henry et al. 2015). The discrepancy suggests that there could be distinct regulatory mechanisms between common glycophyte such as rice and halophyte to adjust the trehalose metabolism under salt stress. Alternatively, the down-regulation of trehalose

biosynthesis genes in *H. tuberosus* might reduce the consumption of glucose.

On the other hand, the expression of three genes encoding callose synthases, as a producer of callose at the cell plate during cytokinesis, was restrained by salt stress. Moreover, two xyloglucan endotransglucosylase proteins (spot 651 and 2668) were significantly reduced under salt stress, which is thought to promote cell expansion by breaking the xyloglucan. In line with the plant phenotype shown in Fig. 1, it is suggested that cell growth and cell division might be inhibited by salt stress, resulting from lowering of the energy expenditure for plant growth and saving it to be used against adversity.

Ribosome activation and translation process

We identified the involvement of a great portion of DEGs (145 genes) related to ribosomes. There were few publications reporting that the ribosome process was directly concerned with the regulatory mechanisms of salt stress. Regarding these DEGs, 127 genes were up-regulated in salt-treated plants, but only 18 genes were down-regulated. Several cellular processes associated with ribosomes were also detected to be highly enriched in many up-regulated DEGs, 129, 119 and 137 genes which were involved in peptide biosynthetic process, and structural constituent of ribosome and ribonucleoprotein complex; all were up-regulated by salt treatment in *H. tuberosus*. 66 genes encoding large and small subunits of ribosomal protein which perform a structural role in ribosomes were all up-regulated by salt treatment. In addition, many mRNA processing- and translation-related genes were detected with higher expression abundance in *H. tuberosus* under salt stress.

In the *Arabidopsis* genome, 249 genes were identified corresponding to 80 (32 small subunit and 48 large subunit) cytoplasmic ribosomal protein (Barakat et al. 2001). Based on our results, a considerable portion of ribosome background transcripts were induced by salinity. As coincidence, transcriptomic profiling of the salt stress response in the halophyte *Beta vulgaris* ssp. *maritima* evinced that 48 of the detected ribosomal protein-encoding mRNAs were differentially expressed under salt stress, but only 11 of them were up-regulated (Skorupa et al. 2016). Comparative proteomic data showed three proteins involved in translation, two ribosomal proteins (spot 41 and 85) and translation initiation factor 3 (spot 2312) were expressed in salt-treated plants with higher abundance. It is demonstrated that translation activation was induced by salt treatment at both the transcript and protein level. Ribosomes and its biogenesis were highlighted since they have essential impact on plant developmental processes, cell growth and survival, as common phenotypes can be observed in ribosomal protein mutants changing the process of translation and protein modification

(Weis et al. 2015). Ribosomal proteins are also involved in controlling organelle trafficking and developmental programs through the regulation of the cellular metabolism (Li et al. 2015). The highly active gene expression of ribosomal behavior demonstrates that the global increase of ribosome remodeling and protein synthesis might conduct a rearrangement of metabolic enzymes synthesis and modulate the plant metabolism to response salt stress.

Oxidoreductase activity

This work also generated a large amount of DEGs that are classified as genes encoding oxidoreductase (429 genes). The dynamics of oxidoreductase activity could affect metabolic processes such as respiration and ATP synthesis, in which they involve multiple oxidation–reduction reactions. For example, 33 genes related to mitochondrial respiratory electron transport and 96 genes encoding proteins involved in ATP synthesis were differentially expressed in *H. tuberosus* under stress. In addition, the transcripts of oxidoreductase were highly represented among DEGs responding to salinity, suggesting that salt stress brings about a significant impact on cellular oxidation–reduction reactions and has profound influence on cellular redox homeostasis. Irregular alterations in the environmental conditions are associated with fluctuations in cellular redox homeostasis (Kocsy et al. 2013; Spoel and van Ooijen 2014). The control of the redox homeostasis is closely affiliated with a complex and redundant antioxidant system, in which enzymes and metabolites are linked in a network of reactions (Potters et al. 2010). In this study, we found the expression of 44 genes encoding antioxidant-associated proteins was significantly affected by salt stress. In particular, four genes encoding glutaredoxin and nine genes encoding peroxidase displayed enhanced expression in salt-treated plants. To be supportive, catalase (spot 2264), a key member of oxidoreductase, was also up-regulated in *H. tuberosus* under salt stress. These data showed that fluctuation of oxidoreductase activity caused by salt treatment might not only give rise to the reprogramming of metabolic process, but also could induce the antioxidant activity to control cellular redox homeostasis, which is consistent with the results from salt-responsive transcriptome profiling of halophyte *Suaeda glauca* (Jin et al. 2016).

Ion binding and ion transport

Genes encoding ion binding-related proteins constitute a large portion of the DEGs with a total of 1041 genes identified (Fig. 6). These DEGs encoding proteins mainly participated in metal ion binding processes, such as of zinc, copper, calcium, iron and magnesium. Metal ions act as cofactors that are necessary for the catalytic activity of the enzymes they bind to (Mohsenzadeh et al. 2011;

Peroza et al. 2013). It is well known that the binding of metal ions can impact many plant metabolic pathways, for example, ROS scavenging and cellular electron transport (Yruela 2013; Pospíšil 2014). In our study, the enrichment of down-regulated genes in ion binding opens the doors to investigations on how ion–protein binding can be used in salt tolerance.

Maintaining of the ion balance plays a significant role in adaptation to salinity conditions of the halophyte species (Zhu 2001). It is critical to exclude excess sodium and chloride and simultaneously ensure the proper concentration of potassium in plant cells (Nieves-Cordones et al. 2016). We found that the expression of 245 genes related to sodium transport was affected by salt stress in *H. tuberosus*. Among these genes, six genes encoding sodium/potassium ATPase, oxaloacetate decarboxylase and NADH dehydrogenase were induced by NaCl treatment, while eight genes encoding transmembrane transport potassium transporter and Kv2 voltage-gated K⁺ channel were down-regulated in salt-treated roots. The high accumulation of sodium transport-related transcripts and

down-regulated potassium transporter-related transcripts emphasized that *H. tuberosus* could remodel ion homeostasis by removing progressive sodium and mitigating the transmembrane transport of potassium.

Protein phosphorylation

Protein kinase-mediated phosphorylation signaling events play important regulatory roles in salt stress response (Rampitsch and Bykova 2012). In this study, based on biological process classification of GO analysis, 425 genes encoding proteins involved in phosphorylation were differentially expressed in *H. tuberosus* under salt stress. Moreover, 353 and 329 DEGs were, respectively, classified into those with protein kinase activity and protein phosphorylation process. In biological terms, most genes were down-regulated, and the reduction of expression in 292 (69%), 267 (75%) and 250 (76%) genes from the three above-mentioned GO terms were triggered by salt treatment. A large portion of DEGs related to phosphorylation

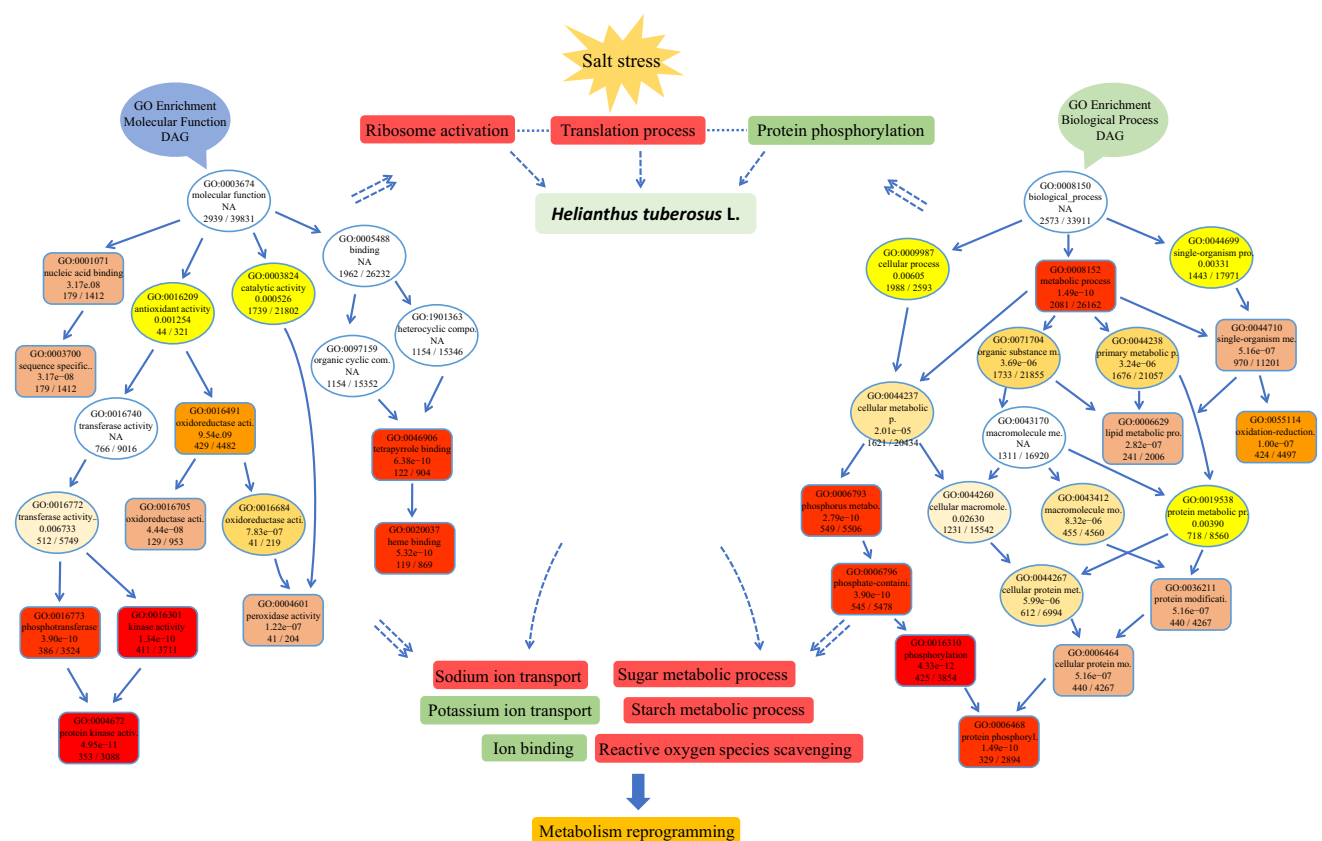


Fig. 9 Schematic view of salt-response molecular-regulatory network in *H. tuberosus*. DAG diagrams were generated by GO database. Salt-responsive GO terms showed in the DAG diagram were elaborated by biological process and molecular function classification. The descrip-

tion and over-represented *P* value of GO biological pathways are displayed in colored ellipse and rectangle. Different colors denote the degree of GO enrichment. The inhibited and induced pathways by salt stress are indicated by green and red code rectangle, respectively

and kinase activity were down-regulated genes in our transcriptomic analysis, suggesting that the overall phosphorylation was inhibited by long-term salt treatment. Comparative phosphoproteomics analysis in *Arabidopsis* and sugar beet showed that numerous phosphoproteins exhibited significant changes under salt stress, which regulated the downstream metabolic process and helped plants to accommodate salt stress (Liu et al. 2015; Yu et al. 2016). Thus, it is plausible that the protein phosphorylation was regulated by salt stress at both the protein and the transcript levels.

Defense and stress-responsive factors

Five genes encoding pathogenesis-related proteins and eight genes encoding protein response to abiotic stress showed significantly increased expression in *H. tuberosus* under salt stress. Four of the genes encode late embryogenesis abundant (LEA) proteins, which act as versatile players in plant adaptation to water-limiting environments. LEA proteins accumulate to high level during the last stages of seed development when desiccation tolerance is acquired in vegetative plant tissues (Olvera-Carrillo et al. 2010, 2011). The overexpression of this group of transcripts might improve the accumulation of LEA proteins and confer tolerance to severe water deficiency caused by salt stress in *H. tuberosus*.

In addition, one salt stress-specific gene encoding monodehydroascorbate reductase (MDHAR) was also up-regulated. MDHAR is an important enzyme of the ascorbate–glutathione cycle, contributing to the scavenging of ROS (Sultana et al. 2012). This result confirms the idea that the antioxidant activity-related genes are activated under salt stress.

Conclusions

This study generates a composite well-annotated transcriptome and proteome of *H. tuberosus* in response to salt stress. De novo transcriptomic assembly produced a total of 293,823 transcripts which were then annotated into 190,567 unigenes. 5432 genes were found to display significant changes in expression under 150 mM NaCl stress. The expression patterns of the DEGs showed that 2165 and 3267 genes were, respectively, shared among up- and down-regulated transcripts in stressed plants. In addition, iTRAQ-labeled proteomic analysis showed that the expression of 43 proteins (19 induced, 24 suppressed) was changed under salt stress. The key gene and protein categories in the modulation of salt stress adaption were identified by GO enrichment. As representatives, rearrangement of synthesis of the metabolic enzymes involved in adjustment of energy supply, osmotic

regulation and ion balance maintenance by actively worked ribosome might contribute to salt tolerance in *H. tuberosus* (Fig. 9). In summary, the salt stress-induced reprogramming of *H. tuberosus* transcriptome and proteome provided not only a framework to understand the molecular mechanisms in response to stress, but also rich genetic information for mining useful genes associated with salt tolerance.

Author contribution statement QP and XY designed the experiments. AZ, DH and HM conducted the experiments. AZ and YW analyzed the data. AZ and QP wrote the manuscript. TZ previewed and revised the manuscript.

Acknowledgements This work was supported by the National Natural Science Foundation of China (No. 31470467) and the Fundamental Research Funds for the Central Universities (2572016DA05 and 2572016AA15).

Compliance with ethical standards

Conflict of interest The authors declare that they have no conflicts of interest.

References

- Abogadallah GM (2010) Antioxidative defense under salt stress. *Plant Signal Behav* 5:369–374
- Anders S, Huber W (2010) Differential expression analysis for sequence count data. *Genome Biol* 11:R106. <https://doi.org/10.1186/gb-2010-11-10-r106>
- Asensi-Fabado MA, Ammon A, Sonnewald U, Munné-Bosch S, Voll LM (2015) Tocopherol deficiency reduces sucrose export from salt-stressed potato leaves independently of oxidative stress and symplastic obstruction by callose. *J Exp Bot* 66:957–971. <https://doi.org/10.1093/jxb/eru453>
- Baack EJ, Whitney KD, Rieseberg LH (2005) Hybridization and genome size evolution: timing and magnitude of nuclear DNA content increases in *Helianthus* homoploid hybrid species. *New Phytol* 167:623–630. <https://doi.org/10.1111/j.1469-8137.2005.01433.x>
- Baiya S, Hua Y, Ekkhara W, Ketudat Cairns JR (2014) Expression and enzymatic properties of rice (*Oryza sativa* L.) monoglucosyl-β-glucosidases. *Plant Sci* 227:101–109. <https://doi.org/10.1016/j.plantsci.2014.07.009>
- Barakat A, Szick-Miranda K, Chang IF, Guyot R, Blanc G, Cooke R, Delseny M, Bailey-Serres J (2001) The organization of cytoplasmic ribosomal protein genes in the *Arabidopsis* genome. *Plant Physiol* 127:398–415. <https://doi.org/10.1104/pp.127.2.398>
- Barker MS, Kane NC, Matvienko M, Kozik A, Michelmore RW, Knapp SJ, Rieseberg LH (2008) Multiple paleopolyploidizations during the evolution of the *Asteraceae* reveal parallel patterns of duplicate gene retention after millions of years. *Mol Biol Evol* 25:2445–2455. <https://doi.org/10.1093/molbev/msn187>
- Barta J, Pátkai GY (2007) Chemical composition and storability of Jerusalem artichoke tubers. *Acta Aliment Hung* 36:257–267. <https://doi.org/10.1556/AAlim.36.2007.2.13>
- Bock DG, Kane NC, Ebert DP, Rieseberg LH (2014) Genome skimming reveals the origin of the Jerusalem Artichoke tuber crop

- species: neither from Jerusalem nor an artichoke. *New Phytol* 201:1021–1030. <https://doi.org/10.1111/nph.12560>
- Boriboonkaset T, Theerawitaya C, Yamada N, Pichakum A, Supai-bulwatana K, Cha-Um S, Takabe T, Kirdmanee C (2013) Regulation of some carbohydrate metabolism-related genes, starch and soluble sugar contents, photosynthetic activities and yield attributes of two contrasting rice genotypes subjected to salt stress. *Protoplasma* 250:1157–1167. <https://doi.org/10.1007/s00709-013-0496-9>
- Chen Q, Zhang MD, Shen SH (2011) Effect of salt on malondialdehyde and antioxidant enzymes in seedling roots of Jerusalem artichoke (*Helianthus tuberosus* L.). *Acta Physiol Plant* 33:273–278. <https://doi.org/10.1007/s11738-010-0543-5>
- de Sá PH, Veras AA, Carneiro AR, Pinheiro KC, Pinto AC, Soares SC, Schneider MP, Azevedo V, Silva A, Ramos RT (2015) The impact of quality filter for RNA-Seq. *Gene* 563:165–171. <https://doi.org/10.1016/j.gene.2015.03.033>
- Draper HH, Hadley M (1990) Malondialdehyde determination as index of lipid peroxidation. *Meth Enzymol* 186:421–431. [https://doi.org/10.1016/0076-6879\(90\)86135-i](https://doi.org/10.1016/0076-6879(90)86135-i)
- Edelman J, Jefford TG (1968) The mechanism of fructosan metabolism in higher plants as exemplified in *Helianthus tuberosus*. *New Phytol* 67:517–531. <https://doi.org/10.1111/j.1469-8137.1968.tb05480.x>
- Ge LF, Chao DY, Shi M, Zhu MZ, Gao JP, Lin HX (2008) Overexpression of the trehalose-6-phosphate phosphatase gene *OsTPP1* confers stress tolerance in rice and results in the activation of stress responsive genes. *Planta* 228:191–201. <https://doi.org/10.1007/s00425-008-0729-x>
- Götz S, Garcia-Gómez JM, Terol J, Williams TD, Nagaraj SH, Nueda MJ, Robles M, Talón M, Dopazo J, Conesa A (2008) High-throughput functional annotation and data mining with the Blast2GO suite. *Nucleic Acids Res* 36:3420–3435. <https://doi.org/10.1093/nar/gkn176>
- Grabherr MG, Haas BJ, Yassour M, Levin JZ, Thompson DA, Amit I, Adiconis X, Fan L, Raychowdhury R, Zeng Q, Chen Z, Mauceli E, Hacohen N, Gnirke A, Rhind N, di Palma F, Birren BW, Nusbaum C, Lindblad-Toh K, Friedman N, Regev A (2011) Full-length transcriptome assembly from RNA-Seq data without a reference genome. *Nat Biotechnol* 29:644–652. <https://doi.org/10.1038/nbt.1883>
- He W, Zhuang HH, Fu YP, Guo LW, Guo B, Guo LZ, Zhang XH, Wei YH (2015) *De novo* transcriptome assembly of a Chinese locoweed (*Oxytropis ochrocephala*) species provides insights into genes associated with drought, salinity, and cold tolerance. *Front Plant Sci* 6:1086. <https://doi.org/10.3389/fpls.2015.01086>
- Henry C, Bledsoe SW, Griffiths CA, Kollman A, Paul MJ, Sakr S, Lagrimini LM (2015) Differential role for trehalose metabolism in salt-stressed maize. *Plant Physiol* 169:1072–1089. <https://doi.org/10.1104/pp.15.00729>
- Higashiyama T (2002) Novel functions and applications of trehalose. *Pure Appl Chem* 74:1263–1269. <https://doi.org/10.1351/pac200274071263>
- Huang ZR, Long XH, Wang L, Kang J, Zhang ZH, Zed R, Liu ZP (2012) Growth, photosynthesis and H⁺-ATPase activity in two Jerusalem artichoke varieties under NaCl-induced stress. *Process Biochem* 47:591–596. <https://doi.org/10.1016/j.procbio.2011.12.016>
- Huang ZR, Zhao L, Chen DD, Liang MX, Liu ZP, Shao HB, Long XH (2013) Salt stress encourages proline accumulation by regulating proline biosynthesis and degradation in Jerusalem artichoke plantlets. *PLoS One* 8:e62085. <https://doi.org/10.1371/journal.pone.0062085>
- Ibrahim MH, Jaafar HZ (2012) Primary, secondary metabolites, H₂O₂, malondialdehyde and photosynthetic responses of *Orthosiphon stamineus* Benth. to different irradiance levels. *Molecules* 17:1159–1176. <https://doi.org/10.3390/molecules17021159>
- Jin HX, Dong DK, Yang QH, Zhu DH (2016) Salt-responsive transcriptome profiling of *Suaeda glauca* via RNA sequencing. *PLoS One* 11:e0150504. <https://doi.org/10.1371/journal.pone.0150504>
- Jung WY, Lee SS, Kim CW, Kim HS, Min SR, Moon JS, Kwon SY, Jeon JH, Cho HS (2014) RNA-Seq analysis and *de novo* transcriptome assembly of Jerusalem artichoke (*Helianthus tuberosus* Linne). *PLoS One* 9:e111982. <https://doi.org/10.1371/journal.pone.0111982>
- Kays SJ, Nottingham SF (2008) Biology and chemistry of the Jerusalem Artichoke: *Helianthus tuberosus* L. CRC Press, Boca Raton
- Kocsy G, Tari I, Vanková R, Zechmann B, Gulyás Z, Poór P, Galiba G (2013) Redox control of plant growth and development. *Plant Sci* 211:77–91. <https://doi.org/10.1016/j.plantsci.2013.07.004>
- Krasensky J, Broyart C, Rabanal FA, Jonak C (2014) The redox-sensitive chloroplast trehalose-6-phosphate phosphatase *AtTPPD* regulates salt stress tolerance. *Antioxid Redox Signal* 21:1289–1304. <https://doi.org/10.1089/ars.2013.5693>
- Kumar R, Ichihashi Y, Kimura S, Chitwood DH, Headland LR, Peng J, Maloof JN, Sinha NR (2012) A high-throughput method for Illumina RNA-Seq library preparation. *Front Plant Sci* 3:202. <https://doi.org/10.3389/fpls.2012.00202>
- Lee BH, Eskandari R, Jones K, Reddy KR, Quezada-Calvillo R, Nichols BL, Rose DR, Hamaker BR, Pinto BM (2012) Modulation of starch digestion for slow glucose release through “togglng” of activities of mucosal α -glucosidases. *J Biol Chem* 287:31929–31938. <https://doi.org/10.1074/jbc.M112.351858>
- Li B, Dewey CN (2011) RSEM: accurate transcript quantification from RNA-Seq data with or without a reference genome. *BMC Bioinform* 12:323. <https://doi.org/10.1186/1471-2105-12-323>
- Li RX, Sun RB, Hicks GR, Raikhel NV (2015) *Arabidopsis* ribosomal proteins control vacuole trafficking and developmental programs through the regulation of lipid metabolism. *Proc Natl Acad Sci USA* 112:E89–E98. <https://doi.org/10.1073/pnas.1422656112>
- Liu ZB, Li Y, Cao HW, Ren DT (2015) Comparative phospho-proteomics analysis of salt-responsive phosphoproteins regulated by the MKK9-MPK6 cascade in *Arabidopsis*. *Plant Sci* 241:138–150. <https://doi.org/10.1016/j.plantsci.2015.10.005>
- Livak KJ, Schmittgen TD (2001) Analysis of relative gene expression data using real-time quantitative PCR and the 2^{(-Delta Delta C(T))} method. *Methods* 25:402–408. <https://doi.org/10.1006/meth.2001.1262>
- Long XH, Huang ZR, Huang YL, Kang J, Zhang ZH, Liu ZP (2010a) Response of two Jerusalem artichoke (*Helianthus tuberosus*) cultivars differing in tolerance to salt treatment. *Pedosphere* 20:515–524. [https://doi.org/10.1016/S1002-0160\(10\)60041-0](https://doi.org/10.1016/S1002-0160(10)60041-0)
- Long XH, Huang ZR, Zhang ZH, Li Q, Zed R, Liu ZP (2010b) Seawater stress differentially affects germination, growth, photosynthesis, and ion concentration in genotypes of Jerusalem artichoke (*Helianthus tuberosus* L.). *J Plant Growth Regul* 29:223–231. <https://doi.org/10.1007/s00344-009-9125-4>
- Ma XY, Zhang LH, Shao HB, Xu G, Zhang F, Ni FT, Brestic M (2011) Jerusalem artichoke (*Helianthus tuberosus*), a medicinal salt-resistant plant has high adaptability and multiple-use values. *J Med Plant Res* 5:1272–1279
- Mao X, Cai T, Olyarchuk JG, Wei LP (2005) Automated genome annotation and pathway identification using the KEGG Orthology (KO) as a controlled vocabulary. *Bioinformatics* 21:3787–3793. <https://doi.org/10.1093/bioinformatics/bti430>
- Miao ZY, Xu W, Li DF, Hu XN, Liu JX, Zhang RX, Tong ZY, Dong JL, Su Z, Zhang LW, Sun M, Li WJ, Du ZL, Hu SN, Wang T (2015) *De novo* transcriptome analysis of *Medicago falcata* reveals novel insights about the mechanisms underlying abiotic stress-responsive pathway. *BMC Genom* 16:818. <https://doi.org/10.1186/s12864-015-2019-x>

- Mohsenzadeh F, Chehregani A, Yousefi N (2011) Effect of the heavy metals on developmental stages of ovule, pollen, and root proteins in *Reseda lutea* L. (Resedaceae). *Biol Trace Elem Res* 143:1777–1788. <https://doi.org/10.1007/s12011-011-9009-x>
- Nieves-Cordones M, Al Shiblawi FR, Sentenac H (2016) Roles and transport of sodium and potassium in plants. *Met Ions Life Sci* 16:291–324. https://doi.org/10.1007/978-3-319-21756-7_9
- Olvera-Carrillo Y, Campos F, Reyes JL, Garcarrubio A, Covarrubias AA (2010) Functional analysis of the group 4 late embryogenesis abundant proteins reveals their relevance in the adaptive response during water deficit in *Arabidopsis*. *Plant Physiol* 154:373–390. <https://doi.org/10.1104/pp.110.158964>
- Olvera-Carrillo Y, Reyes JL, Covarrubias AA (2011) Late embryogenesis abundant proteins: versatile players in the plant adaptation to water limiting environments. *Plant Signal Behav* 6:586–589. <https://doi.org/10.4161/psb.6.4.15042>
- Pang QY, Chen SX, Dai SJ, Chen YZ, Wang Y, Yan XF (2010) Comparative proteomics of salt tolerance in *Arabidopsis thaliana* and *Thellungiella halophila*. *J Proteome Res* 9:2584–2599. <https://doi.org/10.1021/pr100034f>
- Park HJ, Kim WY, Yun DJ (2016) A new insight of salt stress signaling in plant. *Mol Cells* 39:447–459. <https://doi.org/10.14348/molcells.2016.0083>
- Peroza EA, dos Santos Cabral A, Wan X, Freisinger E (2013) Metal ion release from metallothioneins: proteolysis as an alternative to oxidation. *Metallomics* 5:1204–1214. <https://doi.org/10.1039/c3mt00079f>
- Pospíšil P (2014) The role of metals in production and scavenging of reactive oxygen species in photosystem II. *Plant Cell Physiol* 55:1224–1232. <https://doi.org/10.1093/pcp/pcu053>
- Potters G, Horemans N, Jansen MA (2010) The cellular redox state in plant stress biology—a charging concept. *Plant Physiol Biochem* 48:292–300. <https://doi.org/10.1016/j.plaphy.2009.12.007>
- Rampitsch C, Bykova NV (2012) The beginnings of crop phosphoproteomics: exploring early warning systems of stress. *Front Plant Sci* 3:144. <https://doi.org/10.3389/fpls.2012.00144>
- Ranjan A, Ichihashi Y, Farhi M, Zumstein K, Townsley B, David-Schwartz R, Sinha NR (2014) De novo assembly and characterization of the transcriptome of the parasitic weed dodder identifies genes associated with plant parasitism. *Plant Physiol* 166:1186–1199. <https://doi.org/10.1104/pp.113.234864>
- Richter JA, Erban A, Kopka J, Zörb C (2015) Metabolic contribution to salt stress in two maize hybrids with contrasting resistance. *Plant Sci* 233:107–115. <https://doi.org/10.1016/j.plantsci.2015.01.006>
- Rogers C, Thompson T, Seiler GJ (1982) Sunflower species of the United States. National Sunflower Association, Bismark
- Saengthongpinit W, Sajjaanantakul T (2005) Influence of harvest time and storage temperature on characteristics of inulin from Jerusalem artichoke (*Helianthus tuberosus* L.) tubers. *Postharvest Biol Technol* 37:93–100. <https://doi.org/10.1016/j.postharvbio.2005.03.004>
- Shabala S, Wu H, Bose J (2015) Salt stress sensing and early signalling events in plant roots: current knowledge and hypothesis. *Plant Sci* 241:109–119. <https://doi.org/10.1016/j.plantsci.2015.10.003>
- Skorupa M, Gołębiewski M, Domagalski K, Kurnik K, Abu Nahia K, Złoch M, Tretyn A, Tyburski J (2016) Transcriptomic profiling of the salt stress response in excised leaves of the halophyte *Beta vulgaris* ssp. *maritima*. *Plant Sci* 243:56–70. <https://doi.org/10.1016/j.plantsci.2015.11.007>
- Spoel SH, van Ooijen G (2014) Circadian redox signaling in plant immunity and abiotic stress. *Antioxid Redox Signal* 20:3024–3039. <https://doi.org/10.1089/ars.2013.5530>
- Sultana S, Khew CY, Morshed MM, Namasivayam P, Napis S, Ho CL (2012) Overexpression of monodehydroascorbate reductase from a mangrove plant (*AeMDHAR*) confers salt tolerance on rice. *J Plant Physiol* 169:311–318. <https://doi.org/10.1016/j.jplph.2011.09.004>
- Sun Y, Kong X, Li C, Liu Y, Ding Z (2015) Potassium retention under salt stress is associated with natural variation in salinity tolerance among *Arabidopsis* accessions. *PLoS One* 10:e0124032. <https://doi.org/10.1371/journal.pone.0124032>
- Thompson JE, Fry SC (2001) Restructuring of wall-bound xyloglucan by transglycosylation in living plant cells. *Plant J* 26:23–34. <https://doi.org/10.1046/j.1365-3113x.2001.01005.x>
- Trapnell C, Williams BA, Pertea G, Mortazavi A, Kwan G, van Baren MJ, Salzberg SL, Wold BJ, Pachter L (2010) Transcript assembly and quantification by RNA-Seq reveals unannotated transcripts and isoform switching during cell differentiation. *Nat Biotechnol* 28:511–515. <https://doi.org/10.1038/nbt.1621>
- Valluru R, Van Den Ende W (2008) Plant fructans in stress environments: emerging concepts and future prospects. *J Exp Bot* 59:2905–2916. <https://doi.org/10.1093/jxb/ern164>
- Wang XC, Chang LL, Wang BC, Wang D, Li PH, Wang LM, Yi XP, Huang QX, Peng M, Guo AP (2013) Comparative proteomics of *Thellungiella halophila* leaves from plants subjected to salinity reveals the importance of chloroplastic starch and soluble sugars in halophyte salt tolerance. *Mol Cell Proteom* 12:2174–2195. <https://doi.org/10.1074/mcp.M112.022475>
- Weis BL, Kovacevic J, Missbach S, Schleiff E (2015) Plant-specific features of ribosome biogenesis. *Trends Plant Sci* 20:729–740. <https://doi.org/10.1016/j.tplants.2015.07.003>
- Wright L, Wrench P, Hinde RW, Brady CJ (1977) Proline accumulation in tubers of Jerusalem artichoke. *Aust J Plant Physiol* 4:51–60. <https://doi.org/10.1071/PP9770051>
- Yamaguchi T, Blumwald E (2005) Developing salt-tolerant crop plants: challenges and opportunities. *Trends Plant Sci* 10:615–620. <https://doi.org/10.1016/j.tplants.2005.10.002>
- Yates SA, Swain MT, Hegarty MJ, Chernukin I, Lowe M, Allison GG, Ruttink T, Abberton MT, Jenkins G, Skøt L (2014) De novo assembly of red clover transcriptome based on RNA-Seq data provides insight into drought response, gene discovery and marker identification. *BMC Genom* 15:453. <https://doi.org/10.1186/1471-2164-15-453>
- You Q, Yi X, Zhang K, Yao DX, Zhang XY, Wang QH, Zhao XH, Ling Y, Xu WY, Li FG, Su Z (2016) Co-expression network analyses identify functional modules associated with development and stress response in *Gossypium arboreum*. *Sci Rep* 6:38436. <https://doi.org/10.1038/srep38436>
- Young MD, Wakefield MJ, Smyth GK, Oshlack A (2010) Gene ontology analysis for RNA-seq: accounting for selection bias. *Genome Biol* 11:R14. <https://doi.org/10.1186/gb-2010-11-2-r14>
- Yruela I (2013) Transition metals in plant photosynthesis. *Metallomics* 5:1090–1109. <https://doi.org/10.1039/c3mt00086a>
- Yu B, Li JN, Koh J, Dufresne C, Yang N, Qi SS, Zhang YX, Ma CQ, Duong BV, Chen SX, Li HY (2016) Quantitative proteomics and phosphoproteomics of sugar beet monosomic addition line M14 in response to salt stress. *J Proteom* 143:286–297. <https://doi.org/10.1016/j.jprot.2016.04.011>
- Zhang T, Zhu MM, Zhu N, Strul JM, Dufresne CP, Schneider JD, Harmon AC, Chen SX (2016) Identification of thioredoxin targets in guard cell enriched epidermal peels using cysTMT proteomics. *J Proteomics* 133:48–53. <https://doi.org/10.1016/j.jprot.2015.12.008>
- Zhao GM, Liu ZP, Chen MD, Kou WF (2006) Effect of saline aquaculture effluent on salt-tolerant Jerusalem artichoke (*Helianthus tuberosus* L.) in a semi-arid coastal area of China. *Pedosphere* 16:762–769. [https://doi.org/10.1016/S1002-0160\(06\)60112-4](https://doi.org/10.1016/S1002-0160(06)60112-4)
- Zhu JK (2001) Plant salt tolerance. *Trends Plant Sci* 6:66–71. [https://doi.org/10.1016/S1360-1385\(00\)01838-0](https://doi.org/10.1016/S1360-1385(00)01838-0)